Journal of Applied Sciences and Nanotechnology

Journal homepage: jasn.uotechnology.edu.iq

Enhanced Photovoltaic Performance of Silicon Solar Cells via Plasma-Deposited Antireflective Titanium Dioxide Coatings

[1]Saad A. Tuama, [1]Omar A. Abdulrazzaq, [1]Noor A. Nasir*, [1]Alaa H. Saloom, [2]Muatez Mohammed

[1]Renewable Energy and Environment Research Center, Corporation of Research and Industrial Development, Iraq
[2]Department of Chemistry and Physics, Midweastrwan State University, USA

ARTICLE INFO

Article history:
Received: January, 21, 2025
Accepted: October, 04, 2025
Available online: December, 10, 2025

Keywords:
Silicon solar cell,
Titanium dioxide,
DC glow discharge plasma,
Photovoltaic efficiency enhancement

Corresponding Author:
Noor A. Nasir
mae.20.60@grad.uotechnology.edu.iq

ABSTRACT

A cost-effective DC glow discharge plasma system was used to deposit a 75 nm titanium dioxide (TiO_2) antireflective coating on 5 cm2 crystalline silicon solar cells (initial efficiency 10.13%). The plasma-deposited TiO_2 film was nanocrystalline: X-ray diffraction revealed mixed anatase/rutile phases with an average crystallite size of ≈17.6 nm and an optical band gap Eg ≈ 3.5 eV. Atomic force microscopy (AFM) showed a granular surface with average roughness Ra ≈50.7 nm (Rq ≈ 67.7 nm) and grain size ≈ 13.1 nm. Optical reflectance measurements indicated a significant reduction in surface reflectance across the visible spectrum after coating, consistent with enhanced light trapping. Photovoltaic current-voltage (I-V) characterization under standard illumination showed a marked increase in performance: the TiO_2-coated cells exhibited improved short-circuit current density and an enhanced power conversion efficiency (PCE) of 11.56% (up from 10.13%), corresponding to 14.1% relative increase. Notably, the fill factor also improved (from 0.614 to 0.639), reflecting reduced resistive losses in the device. The efficiency gain is attributed to the high refractive index and engineered thickness of the TiO_2 layer, which improve light coupling into the silicon absorber and reduce front-surface reflection. These results demonstrate that a thin (75 nm) plasma-deposited TiO_2 antireflection coating can substantially lower front-surface reflectivity and boost the efficiency of silicon solar cells, offering a straightforward route to higher-performance devices.

https://doi.org/10.53293/jasn.2025.7573.1334, Department of Applied Sciences, University of Technology - Iraq.

1. Introduction

Growing global energy demand highlights the need for advancements in sustainable photovoltaic technologies, focusing on increased efficiency and reduced environmental impact [1]. First-generation crystalline silicon (c-Si) solar cells, which dominate the market, still fall short of their theoretical efficiency limits [2]. One key approach to improve conversion efficiency is minimizing optical losses; in this context, antireflective coatings (ARCs) are crucial for reducing surface reflection and enhancing light absorption [3]. Titanium dioxide (TiO_2) has emerged as an attractive ARC material for c-Si solar cells, owing to its high refractive index, wide band gap, and excellent

chemical stability [4]. Studies report that precisely depositing TiO_2 thin films with optimized quality, thickness, and refractive index in the range of 1.73-2.40, consistently enhances device performance [5]. Furthermore, traditional silicon surface processing often relies on hazardous chemicals (e.g., hydrofluoric acid for etching), motivating the search for more sustainable methods [6]. In this context, research has highlighted environmentally benign TiO_2 coatings and plasma-assisted deposition techniques as promising alternatives to reduce the ecological footprint of solar cell manufacturing while simultaneously improving efficiency [7]. Plasma, a high-energy state of matter, provides unique physical and chemical pathways for material processing, including thin-film deposition for advanced PV devices [8]. In particular, DC glow discharge plasma systems can deposit films with controlled properties at relatively low temperatures, offering a cost-effective fabrication route [9]. Such mild processing conditions are especially relevant, since high-temperature steps can degrade sensitive solar cell structures [10]. Despite these advances, a comprehensive study combining a simple DC glow discharge system and TiO_2 ARC deposition on standard c-Si cells with thorough characterization of the resulting film and its direct impact on PV performance remains limited [11]. Moreover, a systematic benchmarking of this approach against established methods (considering both efficiency gains and environmental benefits from avoiding harsh chemicals) is needed [12]. For example, Cu *et al*. [13] showed that plasma-deposited TiO_2 ARCs increased light absorption and improved solar cell efficiency by up to 15% compared to conventional coatings, while maintaining stability under prolonged testing. Hegedüs *et al*. [14] reported that such TiO_2 coatings reduced reflectance to below 5% across the visible spectrum, leading to higher conversion efficiency and enhanced device longevity. Similarly, Kaur *et al*. [15] demonstrated that optimizing TiO_2 layer thickness and crystallinity significantly increased light absorption, yielding up to an 18% boost in power conversion efficiency (PCE) along with improved durability under weathering. This study addresses these gaps by using a DC glow discharge plasma system to deposit TiO_2 thin films on commercially available c-Si solar cells [16]. The primary objective is to systematically evaluate this low-cost, potentially eco-friendly method for fabricating ARCs and its effect on solar cell performance [17].

This study presents a comprehensive characterization of deposited TiO_2 films. Their crystal structure and surface morphology were analysed using X-ray diffraction (XRD) and scanning electron microscopy (SEM), respectively. Furthermore, the films' optical properties, including transmittance, absorption, and reflectance, were thoroughly investigated. The energy band gap of the TiO_2 films was also determined. Crucially, the photovoltaic parameters of the cells (short-circuit current density, open-circuit voltage, fill factor, and PCE) will be measured before and after coating to quantify any enhancements [18]. The novelty of this work lies in applying a simple DC glow discharge plasma deposition of TiO_2 ARCs onto commercial c-Si solar cells, and in comprehensively evaluating both the performance enhancement and the potential environmental advantages relative to traditional HF-based processes [19]. By correlating the physical and optical properties of the deposited TiO_2 film with the observed efficiency improvement, this study offers valuable insights into the viability of a cost-effective, greener approach to enhancing mainstream photovoltaic technology [20].

2. Experimental setup

The antireflection coating deposition was performed using a custom-built DC glow discharge plasma system (as depicted in **Fig. 1**). This system comprises the following key components: a cylindrical Pyrex plasma chamber , a movable, disc-shaped aluminium anode electrode , a stainless steel cathode electrode assembly incorporating a ceramic crucible, a resistive heater situated beneath the cathode, a DC power supply maximum output voltage V=8 kV, current I=0.5 A, a digital control unit for setting and monitoring plasma parameters, a two-stage rotary vacuum pump (ultimate pressure $<1\times10^{-3}$ mbar) connected to a vacuum line with a manual throttle valve, and a digital Pirani vacuum gauge for pressure monitoring.

2.1 Substrate Cleaning Procedure

Prior to deposition, 1 mm thick glass slides cleaning protocol to ensure surface purity and adhesion. The glass slides were initially rinsed with deionized water. Subsequently, they were immersed in a glass beaker containing deionized water and ultrasonically cleaned for 15 minutes. Following this, the slides were removed from the water, immersed in 99.9% pure ethyl alcohol for 10 minutes, and then dried thoroughly under a flow of high-purity nitrogen gas (99.999%).

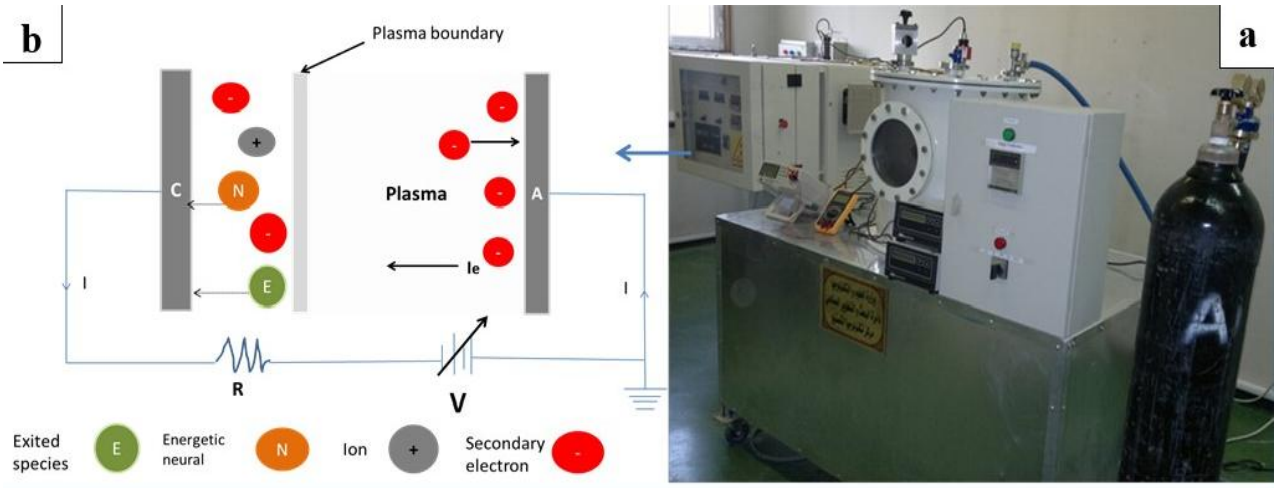

Figure 1: (**a**) Plasma system used for TiO_2 deposition, (**b**) Schematic diagram of the system setup.

2.2 Deposition Procedure

Following a thorough cleaning process, a glass slide was meticulously positioned on the anode electrode using non-contaminating clips. Simultaneously, commercially produced polycrystalline silicon solar cells (from Al-Mansour Factory, with an area of 5 cm^2) were placed adjacent to the glass slide on the anode. This arrangement ensured the concurrent deposition of the TiO_2 antireflection layer onto their front surfaces. Approximately 30 g of high-purity TiO_2 powder (99.9% purity) was loaded into the ceramic crucible, which was integrated into the cathode electrode assembly. The inter-electrode distance between the anode and cathode was maintained at a fixed 2.5 cm.

The plasma chamber was then hermetically sealed, and a rotary vacuum pump evacuated the system to a base pressure of 8.9×10^{-3} mbar. To eliminate residual contaminants, a nitrogen plasma was subsequently generated within the chamber for 30 minutes. This cleaning step was performed at a pressure of 4.5×10^{-1} mbar, with an applied voltage of 1800 V and a current of 0.5 mA. Upon completion of the nitrogen plasma cleaning, argon gas (99.999% purity) was introduced, and the chamber pressure was stabilized at 2.4×10^{-1} mbar. The TiO_2 film deposition then commenced, lasting for 120 minutes. During this period, a DC voltage of 1800 V was applied, and a discharge current of 2.08 mA was maintained. The resistive heater was not engaged during deposition, resulting in an estimated substrate temperature near room temperature (25 °C). The resulting TiO_2 film thickness on the glass slide was measured to be 75 nm.

To evaluate the repeatability of the deposition process, the entire experimental procedure was replicated three times under identical conditions. The observed variation in the TiO_2 film thickness measurements across these runs was within ±5 nm.

3. Experimental Procedure

3.1. Atomic Force Microscopy (AFM)

Atomic Force Microscopy (AFM) was used to investigate the surface morphology of the plasma-deposited TiO_2 ARC on a glass substrate. The resulting AFM image **Fig. 2** revealed a granular surface topography. Quantitative analysis of this topography yielded an average surface roughness (Ra) of 50.71 nm and a root mean square roughness (Rq) of 67.68 nm. The average grain size was determined to be 13.1 nm, indicating the formation of a nanocrystalline TiO_2 film. These roughness values, while higher than those reported for some TiO_2 films deposited via sputtering or sol-gel methods [21], are comparable to studies where increased surface roughness is intentionally engineered to enhance light scattering. The observed surface texture, inherent to the DC glow discharge plasma deposition technique utilized, has implications for light trapping efficiency in solar cell applications. Further optimization of deposition parameters is warranted to balance the benefits of enhanced light scattering with the potential for increased surface recombination. The surface roughness and grain size for the TiO_2 layer from the AFM are summarized in **Table 1**.

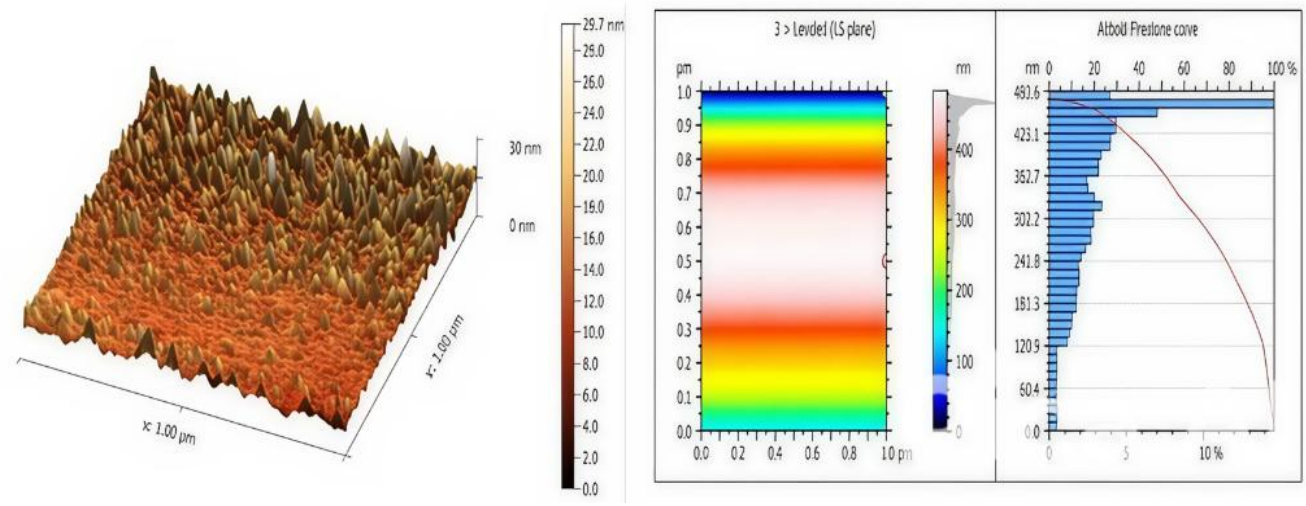

Figure 2: AFM image of the TiO_2 surface, showing topographical features and grain distribution.

Table 1: Surface roughness and grain size of the TiO_2 layer obtained from AFM analysis.

Sample	Average roughness (nm)	Root-mean square	Grain size (nm)
TiO_2	50.71	67.68	13.1

3.2. X-Ray Diffraction (XRD) Analysis

The crystalline structure of the deposited TiO_2 films was investigated using XRD (**Fig. 3**). The XRD patterns revealed the presence of both anatase and rutile phases of TiO_2, indicating a mixed-phase composition of the prepared films. Diffraction peaks observed at 2θ values of 27.5°, 36.1°, 44.3°, and 54.4° were indexed to the (110), (101), (210), and (211) crystallographic planes of the rutile phase (JCPDS card no. 21-1276) [10]. Additionally, diffraction peaks at 53.9°, 62.3°, and 68.7° were assigned to the (105), (204), and (116) crystal planes of the anatase phase (JCPDS card no. 21-1272) [10]. The coexistence of both anatase and rutile phases is further detailed in **Table 2**, which tabulates the XRD pattern characteristics.

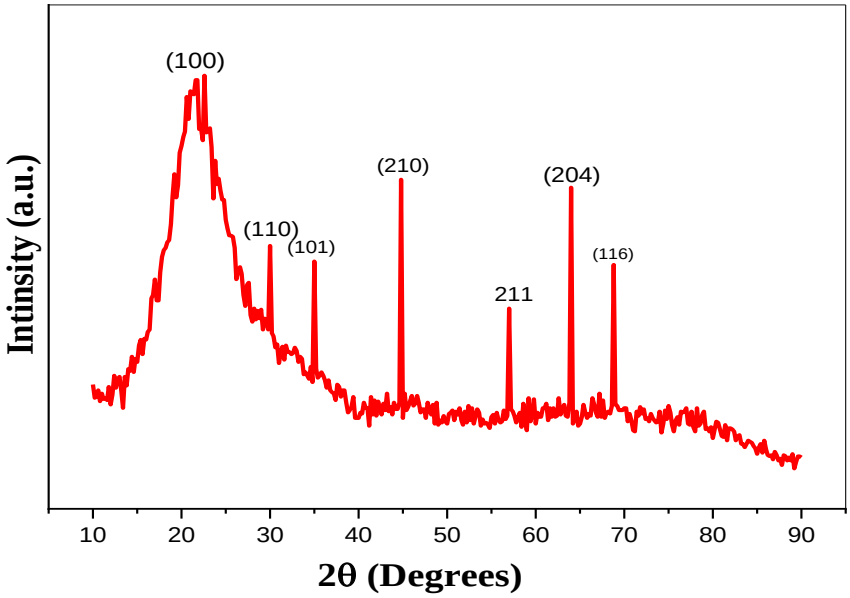

Figure 3: XRD patterns of the TiO_2 film identifying anatase and rutile phases.

Table 2: Structural details of the TiO_2 XRD pattern.

Sample	hkl	Peak position (2θ)	FWHM β (Deg.)	Crystal size D (nm)	Average crystal size (nm)
TiO_2	(110)	27.5°	0.142	0.127	17.58
	(101)	36.1°	7.39	1.545	
	(210)	44.3°	5.59	0.696	
	(211)	54.4°	1.131	53.06	
	(204)	62.3°	0.063	8.033	
	(116)	68.7°	0.1814	2.224	
	(105)	53.9°	3.897	57.40	

The XRD reflection peaks exhibited broadening, which is indicative of small crystallite sizes. The average crystallite size of the TiO_2 film was calculated to be 17.58 nm using the Scherrer equation [22].

The presence of both anatase and rutile phases in TiO_2 films is commonly reported in the literature for films deposited using various techniques, including plasma-based methods [23]. The specific ratio of anatase to rutile can significantly influence the material's properties, particularly its photocatalytic activity [24]. Anatase is considered as an active photocatalyst because it has high effective mass of electrons and holes, which leads to less recombination rate. In addition, the synergistic effect of the anatase-rutile interface can also enhance the charge separation, which can improve the photocatalytic performance in some cases.

The average crystallite size obtained in our study is of 17.58 nm, which lies within the typical range reported in literature for nanocrystalline TiO_2 films when they are deposited at low temperatures [25]. It is known that small crystallite sizes have a larger surface area, which can be beneficial for photocatalysis applications by providing more active sites.

3.3. Field Emission Scanning Electron Microscopic

Fig. 4 shows the image of Field Emission Scanning Electron Microscope (FESEM) of the deposited TiO_2 nano-film. The image reveals a heterogeneous distribution of TiO_2 nanoparticles exhibiting a variety of morphologies with a mean diameter of 107.22 nm. The distribution of particle size is broad and ranges from a few nanometers to several tens of nanometers.

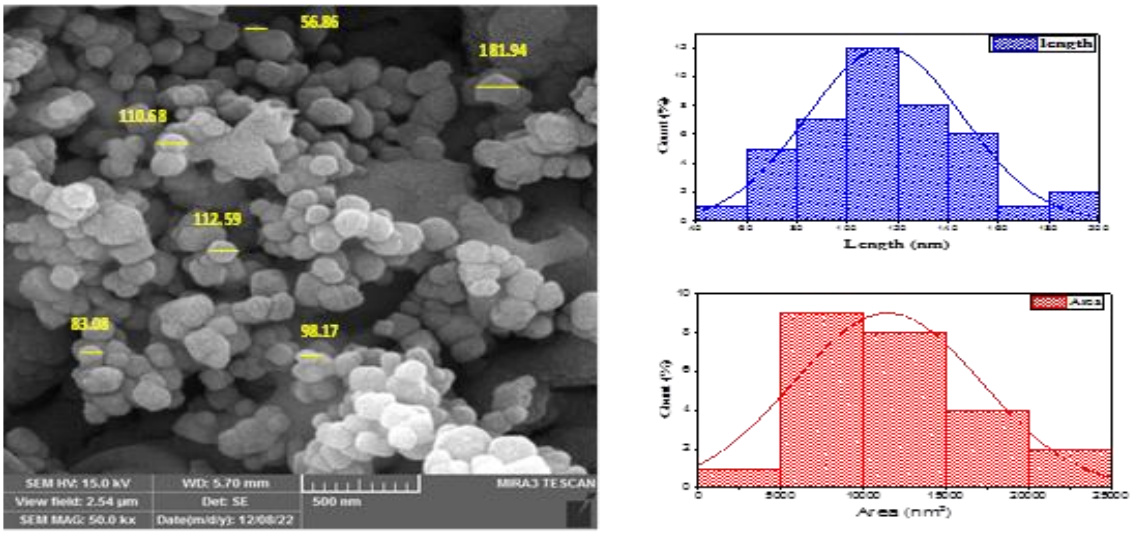

Figure 4: FESEM for TiO_2 nano-thin films.

Moreover, FESEM image indicates a lack of uniformity in particle shapes showing spherical, elongated, and irregularly shaped structures. This morphological diversity likely contributes to the film's antireflective properties through enhanced light scattering and trapping mechanisms across a wider range of incident light angles and

wavelengths [12]. The observed agglomeration of nanoparticles may influence the film's surface roughness, which, in turn, can affect its optical performance by modifying the scattering behavior and potentially increasing the effective refractive index.

The surface morphology of the TiO_2 nano-thin film, as revealed by FESEM, plays a crucial role in its effectiveness as an ARC for silicon solar cells. The broad particle size distribution and the variety of particle shapes can enhance light scattering, redirecting incident light that would otherwise be reflected back into the silicon substrate for absorption and conversion into electricity. This is particularly important for broadband antireflection, aiming to reduce reflection across a wider range of the solar spectrum. Particle sized obtained from the FESEM images for TiO_2 nano-thin films are summarized in **Table 3**.

Table 3: Particles dimensions from the FESEM images for TiO_2 nano-thin films.

Sample thickness (nm)	Size or particles (nm)	Average size (nm)
75	56.86 181.94 110.68 112.59 98.17 83.08	107.22

3.4. Optical Properties

3.4.1. Transmittance Spectra

Transmittance measurements were conducted within the wavelength range of 300–800 nm for the TiO_2 coating deposited on the glass slide. The results revealed that transmittance increased gradually with wavelength up to a certain point, after which it began to decrease. **Fig. 4** illustrates the transmittance as a function of wavelength, highlighting the optical behavior of the TiO_2 layer within this spectral range.

The transmittance spectra of the TiO_2 coating exhibit a wavelength-dependent behavior within the 300-800 nm range. Initially, transmittance increases gradually with increasing wavelength, indicating greater transparency to longer wavelengths. However, beyond a critical point, transmittance decreases, suggesting absorption and scattering effects within the TiO_2 layer. This wavelength-dependent behavior is crucial for evaluating the coating's performance in applications like solar cells, where high transmittance in the visible and near-infrared regions is essential for maximizing light absorption by the underlying photovoltaic material. **Fig. 5** illustrates the transmittance as a function of wavelength, highlighting the optical behavior of the TiO_2 layer within this spectral range [12].

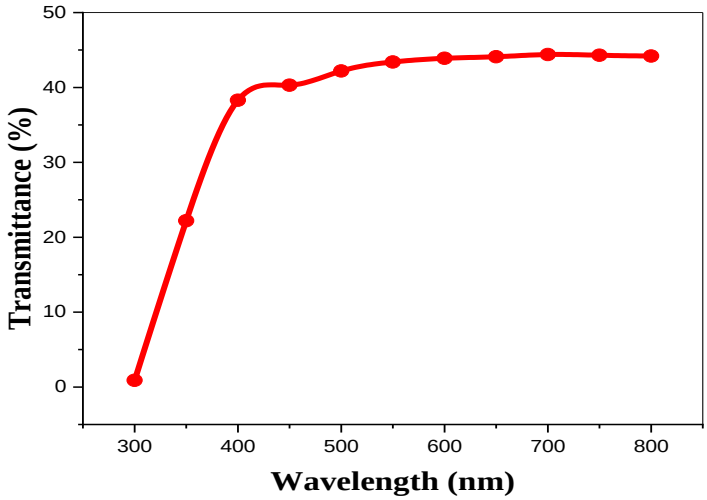

Figure 5: Transmittance spectra of the TiO_2 coating as a function of wavelength.

3.4.2. The Reflectance Spectra

The graph presented in **Fig. 6** compares the reflectance of a surface with and without a thin TiO_2 coating across a specific wavelength range. This type of analysis is crucial in numerous applications, especially in optics and optical coatings, where controlling reflectance plays a vital role in enhancing the efficiency of optical devices. The figure demonstrates that the uncoated surface reflects a significant portion of incident light, particularly in the short wavelength region (blue and violet). This is characteristic behavior for many surfaces, where a significant portion of incident light undergoes reflection from their top layer. After a TiO_2 coating, a significant decrease in reflectance is observed across most of the wavelength range. This reduction indicates that the coating effectively minimizes the amount of reflected light, thereby increasing the amount of light transmitted into the material. Interestingly, the coating reduces reflectance to negative values in certain spectral regions. This phenomenon does not suggest light emission from the surface. Instead, it points to interference between reflected and transmitted light waves. This interference occurs because of the ultra-thin (75 nm) TiO_2 layer, leading to a mutual cancellation of these waves [19].

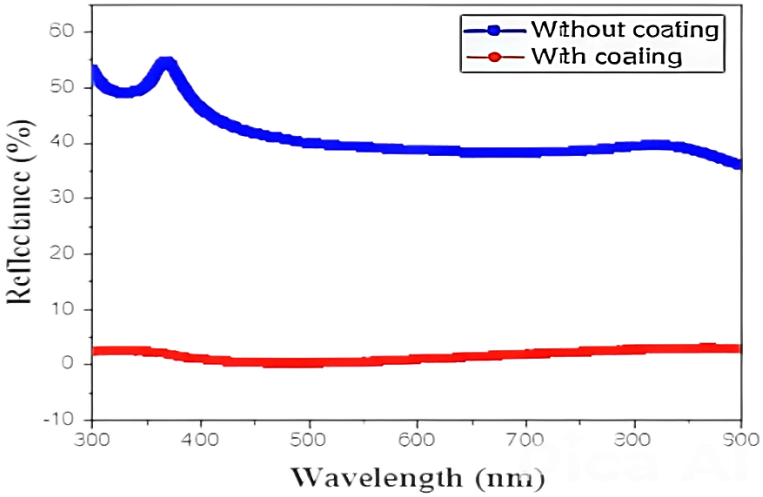

Figure 6: The Reflectance Spectra for TiO_2 nano-thin films.

3.4.3. Optical Energy Gap

The band gap of TiO_2 was determined by plotting the curve $(\alpha h\nu)^2$ as a function of photon energy. **Fig. 7** illustrates this relationship, where the intersection of the extended straight portion of the curve with the photon energy axis represents the value of the direct band gap. For TiO_2, the band gap was found to be 3.5 eV. The band gap results are consistent with values reported in literature.

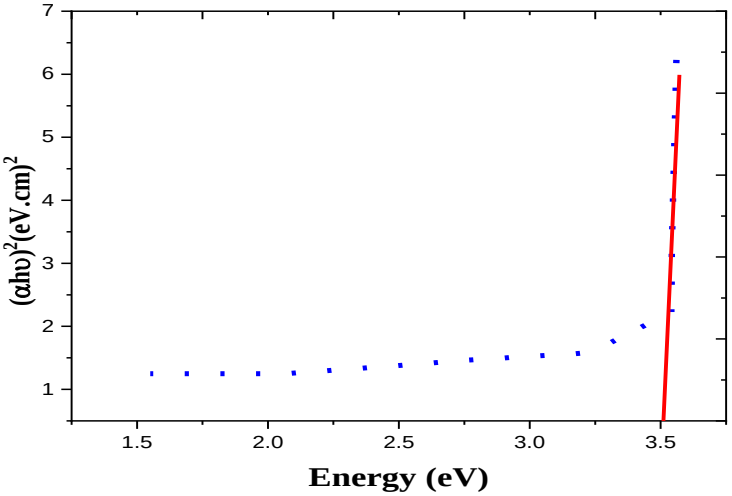

Figure 7: Plot of $(\alpha h\nu)^2$ versus photon energy for TiO_2, showing a direct band gap of 3.5 eV.

The calculation of the band gap was performed using **Eq. (1)** [19]:

$$\alpha h\nu = A\,(h\nu - Eg)^{r} \quad (1)$$

Where, α is the absorption coefficient, h is the Planck's constant, ν is the frequency of the incident light, A is a material-dependent constant, Eg is the optical band gap, and r is a coefficient determined by the material type and the nature of the electronic transition.

The calculated band gap value is consistent with that reported in literature, where the range of allowed transitions of TiO_2 nanostructure usually fall in between 3.2 and 3.29 eV. The band gap extrapolation was performed using **Eq. (1)** [19] that relates absorption coefficient (α), photon energy (hν), and the optical band gap (Eg). TiO_2 energy gap values are presented in **Table 4**.

Table 4: Energy gap values corresponding to TiO_2.

Sample	Energy gap (E_g)
TiO_2	3.5 eV
TiO_2 nanostructure	allowed transition (3.2 - 3.29) eV [12]

3.5. Electrical Properties

The photovoltaic performance parameters of the silicon solar cell were investigated with and without plasma deposition of TiO_2 antireflection coating. The results are presented in **Table 5**, while **Fig. 8** illustrate the I-V curves of the solar cell before and after the antireflection deposition. I-V characterization demonstrated a substantial 14.12% relative increase in PCE, improving from 10.13% to 11.56%. **Table 5** summarizes the performance enhancement of a solar cell following the application of an anti-reflective coating. Notably, efficiency increased from 10.13% to 11.56%. This improvement was primarily driven by an improved fill factor (0.614 to 0.639) and a slight increase in open-circuit voltage V_{OC} (548.4×10^{-3} V to 562.2×10^{-3} V). While a minor decrease in short-circuit current I_{SC} was observed (162.481×10^{-3}A to 160.809×10^{-3} A), the overall power output increased.

Table 5: Solar cell photovoltaic parameters.

PV Test	Before coating	After coating
V_{OC}	548.4×10^{-3} V	562.2×10^{-3} V
I_{SC}	162.481×10^{-3}A	160.809×10^{-3} A
Vm	405.1×10^{-3} V	425.1×10^{-3} V
Im	134.958×10^{-3} A	135.968×10^{-3} A
Pm	54.68×10^{-3} W	57.80×10^{-3} W
FF	0.614	0.639
PCE	10.13%	11.56%
Rs	508.0×10^{-3} Ω	450.3×10^{-3} Ω
Rsh	6.71×10^{3} Ω	228.33×10^{-3} Ω

The TiO_2 ARC's high transparency and refractive index explain the Jsc enhancement. This film's optical bandgap (3.5 eV) means it is transparent throughout the visible spectrum, so it does not absorb useful solar photons. Experimentally we saw much higher transmittance and lower reflectance after coating, indicating a reduction in reflection losses and improved light absorption. Consistent with these findings, our coated cells exhibit higher Jsc (and thus higher PCE) because the high-index (~2.3–2.4) of TiO_2 layer at roughly quarter-wave thickness minimizes front-face reflection. The result is more photons reaching the Si absorber. V_{OC} and FF are less directly affected by the coating (being dominated by device resistances), so the ARC's main effect is in raising Jsc.

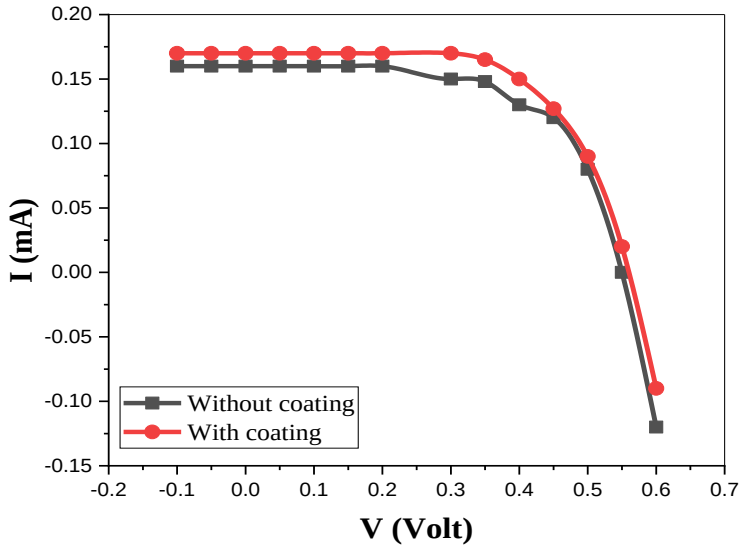

Figure 8: I-V curves of the silicon solar cell with and without TiO_2 plasma deposition.

The resistances Rsh (shunt resistance) and Rs (series resistance) play crucial roles in the overall performance of solar cells. Low Rsh causes leakage currents, while high Rs results in a decreasing current flow. As shown in **Table 4**, The Rs decreased from 508.0 mΩ to 450.3 mΩ after depositing the TiO_2 antireflection layer, indicating enhanced charge transport and reduced resistive losses. In contrast, the Rsh dropped significantly from 6.71 kΩ to 228.33 Ω, suggesting potential defects or leakage pathways introduced during the coating process. Our results illustrate the classic roles of series and shunt resistances. A low Rs minimizes voltage drop under load (preserving FF), while a high Rsh (little leakage) preserves V_{OC} and FF [26][27]. We observed a slight decrease in Rs after coating, implying marginally improved conduction (perhaps via the TiO_2 surface layer or contact coverage). Importantly, theory and experiments both show that devices with low Rs and high Rsh achieve the best FF and V_{OC}, whereas a low Rsh depresses V_{OC} and FF [27]. In our case, the slight Rs improvement should benefit FF, but the dramatic Rsh loss would suppress both V_{OC} and FF. Thus, the net efficiency increase (14%) is driven primarily by photocurrent gains, while the new leakage paths limit FF, which is consistent with observing a higher Jsc but only a modest FF in the coated device.

14.12% relative PCE gain (from 10.13% to 11.56%) is modest compared to some reports of TiO_2 ARCs. For example, Hocine *et al*. showed an ~27% efficiency increase on mc-Si by Atmospheric Pressure Chemical Vapor Deposition (APCVD) TiO_2 deposition, and Lien *et al*. (2006) reported a ~39.5% boost using a triple-layer SiO_2/TiO_2 stack [28]. More recently, Alkallas *et al*. (2024) achieved ≈19–20% PCE on crystalline Si with a sputtered TiO_2:Al_2O_3 blend [29]. These disparities reflect differences in coating methods and film properties: high-index, vacuum-deposited TiO_2 films tend to suppress reflectance more completely (and thus drive larger Jsc gains) than simpler spin-coated sols, but at greater process complexity [28][29]. In this light, our ~14% improvement is consistent with other single-layer, solution-derived TiO_2 ARCs: it yields a significant Jsc gain from reduced reflectance but does not approach the extreme enhancements seen with multilayer or nanostructured ARCs. Lungu *et al*. also noted that adding thicker TiO_2 buffer layers can increase Rs and lower FF [30], whereas we saw the opposite trend in Rs. These results underscore the effectiveness of anti-reflective coatings in enhancing solar cell performance [12].

Despite the overall improvement, the significant drop in Rsh suggests potential defects or leakage pathways introduced during the coating process that limited the full potential of the optical gains. Future work must address these shunting defects (e.g., by optimizing the TiO_2 deposition) to fully realize the optical gains and further enhance the photovoltaic performance.

4. Conclusions

This study successfully demonstrated the efficacy of employing a thin (75 nm) TiO_2 antireflection coating, deposited via a cost-effective DC glow discharge plasma technology, to enhance the efficiency of p-n junction

silicon solar cells. The optimized deposition process yielded a macroscopically uniform TiO_2 layer that facilitated a notable increase in PCE from 10.13% to 11.56%. Structural (XRD) and surface morphological (AFM, FESEM) characterizations revealed a nanocrystalline, mixed-phase TiO_2 film with a specific surface roughness that contributed to improved light trapping. This optical characterization highlights the favourable transparency and refractive index of the TiO_2 coating, which are crucial for reducing surface reflectivity and maximizing light absorption within the silicon absorber layer. The significance of these findings extends beyond a simple efficiency gain. In the context of sustainable development and cleaner energy production, enhancing the performance of existing silicon solar cell technology through cost-effective and potentially less environmentally impactful methods like plasma deposition is crucial. Compared to traditional chemical vapor deposition or sputtering techniques, DC glow discharge plasma systems often require less complex infrastructure and can operate at lower temperatures, potentially reducing energy consumption and hazardous waste generation. The use of TiO_2, an abundant and non-toxic material, further aligns with green chemistry principles.

Conflict of Interest

The authors declare that they have no conflict of interest.

Editorial Transparency

Omar A. Abdulrazzaq is the Editor of the Journal of Applied Sciences and Nanotechnology. Despite this role, the peer review process and the final decision were conducted independently, ensuring that his editorial role did not influence the outcome in any way.

References

[1] S. Sargunanathan, A. Elango, and S. T. Mohideen, "Performance enhancement of solar photovoltaic cells using effective cooling methods: A review," *Renew. Sustain. Energy Rev.*, vol. 64, pp. 382–393, 2016.

[2] A. S. Naji, H. H. Enawi, and A. A. A. Mahmood, "Renewable Energy Resources in Iraq: A Review," *J. Univ. Babylon Eng. Sci.*, vol. 31, no. 4, pp. 1–14, 2023, [Online]. Available: https://www.journalofbabylon.com/index.php/JUBES/article/view/4661

[3] M. Sharma, J. Panigrahi, and V. K. Komarala, "Nanocrystalline silicon thin film growth and application for silicon heterojunction solar cells: a short review," *Nanoscale Adv.*, vol. 3, no. 12, pp. 3373–3383, 2021.

[4] R. A. Morgan, *Plasma etching in semiconductor fabrication*. Elsevier Science Pub. Co. Inc., New York, NY, 1985.

[5] R. A. Saleh, O. N. Salman, and M. O. Dawood, "Physical investigations of titanium dioxide nanorods film prepared by hydrothermal technique," *J. Appl. Sci. Nanotechnol.*, vol. 1, no. 3, pp. 32–41, 2021.

[6] R. Sagar and A. Rao, "Increasing the silicon solar cell efficiency with transition metal oxide nano-thin films as anti-reflection coatings," *Mater. Res. Express*, vol. 7, no. 1, p. 16433, 2020.

[7] R. O. Abdulsada and T. A. A. Hassan, "Synthesis of TiO_2 thin films nanoparticles with different layers using simple sol-gel method," *Iraqi J. Sci.*, pp. 4425–4429, 2021.

[8] I. F. Hasan, K. S. Khashan, and A. A. Hadi, "Study of the effect of laser energy on the structural and optical properties of TiO_2 NPs prepared by PLAL technique," *J. Appl. Sci. Nanotechnol.*, vol. 2, no. 1, pp. 11–19, 2022.

[9] H. J. A. Karim and G. H. Mohammed, "Effect of Transition Metal Dopant on the Electrical Properties of ZnO-TiO_2 Films Prepared by PLD Technique," *Iraqi J. Phys.*, vol. 19, no. 49, pp. 75–81, 2021.

[10] R. E. Klinger, "Thin film deposition technologies, and structure/property relationships applied to solid state ionic conductors," *Solid State Ionics*, vol. 52, no. 1–3, p. 249, 1992.

[11] R. R. Mahdi and M. K. Abood, "Advanced photovoltaic applications of CdO films prepared by pulsed laser ablation on porous silicon," *J. Appl. Sci. Nanotechnol.*, vol. 4, pp. 53–64, 2024.

[12] N. A. Nasir, K. M. Shabeeb, A. K. Hassan, and S. M. Mahmood, "Structural, optical, and electrical characteristics of Titanium Dioxide Thin films prepared by Pulsed Laser Deposition," *Iraqi J. Ind. Res.*, vol. 10, no. 3, pp. 1–10, 2023.

[13] D. T. Cu, J. L. Ho, K. Y. Ko, K. W. Lu, M. C. Li, H. P. Chen, *et al.*, "Effect of insertion layers on the environmental stability of TiO_2/SiO_2 anti-reflective coatings on PMMA substrates," *Surf. Coatings Technol.*, vol. 512, p. 132375, 2025.

[14] N. Hegedüs, K. Balázsi, and C. Balázsi, "Silicon nitride and hydrogenated silicon nitride thin films: A

review of fabrication methods and applications," *Materials (Basel).*, vol. 14, no. 19, p. 5658, 2021.

[15] G. Kaur, A. J. Olivares, and P. Roca i Cabarrocas, "Development of n-Type, Passivating Nanocrystalline Silicon Oxide Films via Plasma-Enhanced Chemical Vapor Deposition," in *Solar*, MDPI, 2024, pp. 162–178.

[16] I. Benammar, R. Salhi, J.-L. Deschanvres, and R. Maalej, "Study of the physico-chemical properties of sol-gel (Er, Yb) doped TiO_2 nanoparticles prepared with a novel protocol," *J. Appl. Sci. Nanotechnol.*, vol. 3, no. 2, pp. 1–17, 2023.

[17] F. H. Kamil, S. K. A. Barno, F. Shems, A. Jihad, and A. S. Abbas, "Photocatalytic degradation of sulfamethoxazole from a synthetic pharmaceutical wastewater using titanium dioxide (TiO_2) powder as a suspended heterogeneous catalyst," *Iraqi J. Ind. Res.*, vol. 10, no. 1, pp. 26–33, 2023.

[18] O. Durante, C. Di Giorgio, V. Granata, J. Neilson, R. Fittipaldi, A. Vecchione, *et al.*, "Emergence and evolution of crystallization in TiO_2 thin films: A structural and morphological study," *Nanomaterials*, vol. 11, no. 6, p. 1409, 2021.

[19] B. V. S. Praveen, P. Madhuri, R. K. Verma, A. Ashok, and S. G. Deshmukh, "Metal Oxide Thin Films: A Comprehensive Study of Synthesis, Characterization and Applications," in *Thin Film Nanomaterials: Synthesis, Properties and Innovative Energy Applications*, Bentham Science Publishers, 2024, pp. 166–198.

[20] J. N. P. K. Chintala, S. Arumugam, R. S. Dubey, S. Saravanan, and K. Srinivasarao, "Empowerment of Photonics in Thin Film Amorphous Silicon Solar Cells," *Eng. Sci.*, vol. 33, p. 1370, 2025.

[21] A. Chacko, E. Hack, S. Lohde, R. Bucher, O. Yildirim, A. M. Müller, *et al.*, "On tailoring structural and optoelectronic properties of TiO_2 thin films synthesized via'room'temperature high power impulse magnetron sputtering (HiPIMS)," *J. Phys. Energy*, 2025.

[22] M. A. Alam, S. Ahmed, R. K. Bishwas, S. Mostofa, and S. A. Jahan, "X-ray crystallographic diffraction study by whole powder pattern fitting (WPPF) method: Refinement of crystalline nanostructure polymorphs TiO_2," *South African J. Chem. Eng.*, vol. 51, pp. 68–77, 2025.

[23] J. D. Lawton, S. A. Thornley, S. J. Wakeham, M. J. Thwaites, V. Stolojan, and M. A. Baker, "Reactive remote plasma sputtering of TiO_x thin films and controlled growth of textured single-phase rutile using rf substrate biasing," *Surf. Coatings Technol.*, vol. 476, p. 130247, 2024.

[24] R. Kawakami, T. Matsumoto, S. Yanagiya, A. Shirai, Y. Nakano, and M. Niibe, "Enhanced Photocatalytic Activity of Anatase/Rutile-Mixed Phase Titanium Dioxide Nanoparticles Annealed with Polyethylene Glycol at Low Temperatures in Aluminum Foil-Covered Combustion Boats," *Phys. status solidi*, vol. 222, no. 2, p. 2400478, 2025.

[25] W. Song, Q. Jiang, X. Xie, A. Brookfield, E. J. L. McInnes, P. R. Shearing, *et al.*, "Synergistic storage of lithium ions in defective anatase/rutile TiO_2 for high-rate batteries," *Energy Storage Mater.*, vol. 22, pp. 441–449, 2019.

[26] M. Kumar and S. Kumar, "24.13% efficient TiO_2/i–a–Si: H/p–c–Si heterojunction solar cell by AFORS-HET numerical simulation," *Opt. Quantum Electron.*, vol. 55, no. 5, p. 441, 2023.

[27] J. Wang, X. Zou, J. Zhu, J. Cheng, D. Chen, X. Bai, *et al.*, "Effect of optimization of TiO_2 electron transport layer on performance of perovskite solar cells with rough FTO substrates," *Materials (Basel).*, vol. 13, no. 10, p. 2272, 2020.

[28] A. Afzal, A. Habib, I. Ulhasan, M. Shahid, and A. Rehman, "Antireflective self-cleaning TiO_2 coatings for solar energy harvesting applications," *Front. Mater.*, vol. 8, p. 687059, 2021.

[29] F. H. Alkallas, S. M. Alghamdi, G. V. Kaliyannan, R. Gunasekaran, R. Rathanasamy, A. B. G. Trabelsi, *et al.*, "Enhanced efficiency of mono-crystalline Si solar cells utilizing RF sputtered TiO_2–Al_2O_3 blended anti-reflection coating for optimal sunlight transmission and energy conversion," *Ceram. Int.*, vol. 50, no. 9, pp. 14865–14877, 2024.

[30] J. Lungu, N. Stefan, G. Prodan, A. Georgescu, A. Mandeş, V. Ciupină, *et al.*, "Characterization of spin-coated TiO_2 buffer layers for dye-sensitized solar cells," *Dig. J. Nanomater. Biostructures*, vol. 10, no. 3, pp. 967–976, 2015.